Performance and Stability of Halide Perovskite Solar Cells in Bahir Dar Climatic Conditions

Getnet M. Meheretu[1,2,6,7(✉)], Getasew A. Wubetu[1], Bart Roose[6], Amare Kassew[4], Hailu Shimels[5], Seifu A. Tilahun[3], Elizabeth M. Tennyson[6], and Samuel D. Stranks[6,7]

[1] Energy Center, Bahir Dar Institute of Technology, Bahir Dar University, Bahir Dar, Ethiopia
[2] Department of Physics, College of Science, Bahir Dar University, Bahir Dar, Ethiopia
[3] Faculty of Civil and Water Resources Engineering, Bahir Dar Institute of Technology, Bahir Dar University, Bahir Dar, Ethiopia
[4] Faculty of Electrical and Computer Engineering, Bahir Dar Institute of Technology, Bahir Dar University, Bahir Dar, Ethiopia
[5] Faculty of Mechanical and Industrial Engineering, Bahir Dar Institute of Technology, Bahir Dar University, Bahir Dar, Ethiopia
[6] Department of Physics, Cavendish Laboratory, University of Cambridge, Cambridge, UK
[7] Department of Chemical Engineering and Biotechnology, University of Cambridge, Cambridge, UK

Abstract. Perovskite solar cells are one of the most promising solar cell technologies, showing rapid development in power conversion efficiency (PCE). In this work, the performance and stability of triple-cation perovskite solar cells under continuous outdoor illumination in Bahir Dar climatic conditions and also the luminescence properties using steady-state photoluminescence (PL) spectroscopy has been studied. The work is conducted to study the electrical characterisation of the device under investigation in outdoor testing under ambient conditions to study the open-circuit voltage, short-circuit current density, fill factor, and efficiency of the device and obtained a PCE of above 16%, and a fill factor of above 60% with strong PL peak emission at 757 nm.

Keywords: Perovskite solar cells · Stability · Performance · Optoelectronic properties · Band gap tenability · PL spectroscopy

1 Introduction

Perovskite solar cells are one of the promising solar cells that attracted great attention for many researchers in the last few years. Recent studies show that single junction perovskite photovoltaic (PV) cells achieved power-conversion efficiency (PCE) of 25.5% and planar silicon/perovskite tandem cells achieved a PCE of 29% [1–4].

The performance and stability of the perovskite solar cells depend on the charge carrier recombination, band structure, compositional engineering, and external environmental exposures [5, 6]. The operation of a solar cell is governed by semiconductor

M. L. Berihun (Ed.): ICAST 2021, LNICST 412, pp. 554–564, 2022.
https://doi.org/10.1007/978-3-030-93712-6_37

physics; under illumination electrons and holes are generated and subsequently extracted and transported through the external circuit. The band gap ultimately governs the achievable PCE through the Shockley-Queisser (SQ) limit [1, 5]. The main electrical parameters that are used to characterise the performance of perovskite solar cells are: the power-conversion efficiency (PCE), short-circuit current density (J_{sc}), fill factor (FF), and open-circuit voltage (V_{oc}) [5]. The current density when there is no bias voltage is referred to as the short-circuit current density, while the voltage for which no current is extracted is termed as the open circuit voltage, i.e. $J\ (V = 0) = J_{sc}$, $V\ (J = 0) = V_{oc}$. The PCE of a solar cell can be expressed as [7]

$$P_{CE} = \frac{I_{out}}{I_{in}} = \frac{V_m J_m}{I_{in}} \tag{1}$$

where V_m and J_m are the voltage and current density respectively at the maximum power point density, I_{in} the power in the incident light and I_{out} the generated electrical power.

The FF of a solar cell describes the squareness of the J-V curve, which is determined by series and shunting resistance and is expressed as [8]

$$FF = \frac{V_m J_m}{V_{oc} J_{sc}} \tag{2}$$

Therefore, the PCE is can be expressed in the form [9]:

$$P_{CE} = \frac{V_m J_m}{I_{in}} = \frac{FF \times V_{oc} \times J_{sc}}{I_{in}} \tag{3}$$

Perovskite solar cells use hybrid organic-inorganic lead (Pb) halide perovskite as the light absorbing material. Perovskites have an ABX_3 crystal structure (Fig. 1), where A is a large cation (typically methylammonium (CH_3NH_3), formamidinium ($CH(NH_2)_2$) or cesium), B a divalent metal cation (Pb) and X is a halide anion (usually I or Br). The crystal structure and stability of perovskites can be determined by the Goldschmidt tolerance factor (t) and expressed as [10–14].

$$t = \frac{1}{\sqrt{2}} \frac{(R_A + R_X)}{(R_B + R_X)} \tag{4}$$

where R_A, R_B, R_X are radii of the ions A, B, and X respectively.

The most reproducible and highest performing cells employ mixed cation, mixed anion configurations which use a mixture of formamidinium and methylammonium as the monovalent cations as well as inorganic cesium. The triple cation perovskite configuration resulting from this composition posseses high thermal stability, contain less phase impurities and are less sensitive to processing conditions.

Halide perovskites have excellent optoelectronic properties, which makes them ideal for solar cell applications. The weak exciton binding energy and a high dielectric constant enable the dissociation of excitons to free electrons and holes. Furthermore,

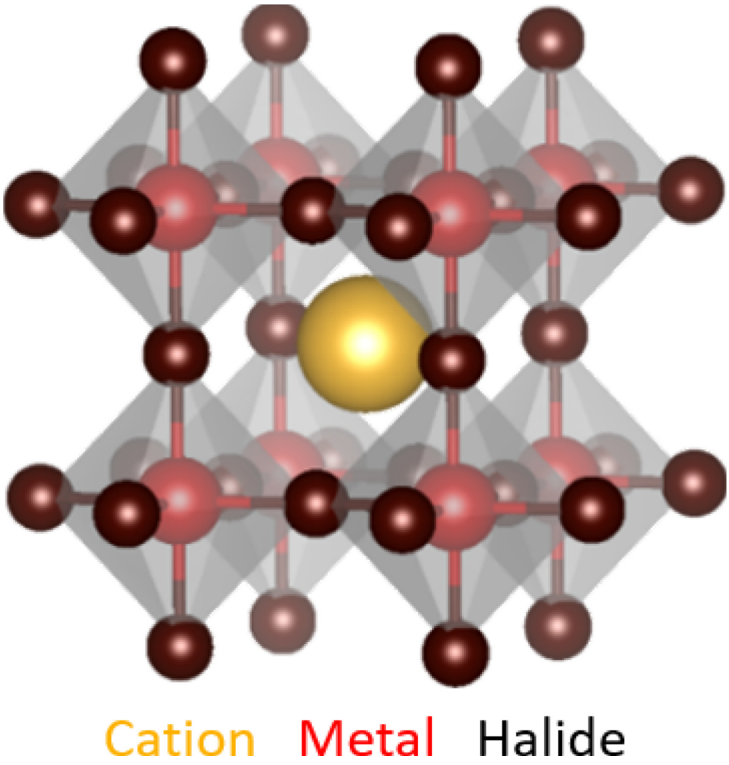

Fig. 1. Crystal structure of perovskites [adapted from reference [15, 16].

halide perovskites possess a tuneable direct bandgap, have a large absorption coefficient, low defect density, small Urbach energy, and long diffusion length [17–19].

Perovskites have excellent optoelectronic properties; however, it has intrinsic chemical instability of the absorber layer leading to degradation of the electronic properties [20]. There are also extrinsic instabilities that are usually caused by ions migration, exposure to visible and UV light, heat [21, 22], humidity and oxygen. Studies show that compositional engineering of the aforementioned mixed cation, mixed anion configurations perovskite can drastically increase stability. In addition, the electron transport layer (ETL), and hole transport layer (HTL) can promote instabilities stabilities as well [23, 24]. The stability of the perovskite solar cell can be improved using hybrid organic-inorganic cations of mixed halide with appropriate encapsulation. Passivation treatment with organic materials can reduce the defects in the perovskite surface and inhibits moisture entry into the device that can enable the device to better withstand degradation [15, 25–30].

Cesium based triple cations have high PCE and higher bandwidth than their corresponding non-cesium containing perovskites, and have attracted great attention for perovskite-based tandem cells for strong absorption of light in the whole solar spectrum. These cations essentially contains (CH_3NH_3), ($CH(NH_2)_2$ as monovalent organic cations, and cesium as inorganic cation to form triple cation [31, 32].

Since its emergence, perovskite solar cells show a rapid development that can surpass the solar technology performance within ten years and has achieved a PCE of 25.2%. In addition to its rapid enhancement in performance, its intrinsic optoelectronic properties, low-cost and ease of production have attracted great attention [33, 34]. Nevertheless stability is still the main challenge that hinders the commercialization of perovskite solar cell technology.

There is a possibility to improve the performance by changing the composition, and the device architecture [10, 12, 34, 35]. Researchers conducted on the degradation of PSCs shows that cells stored in the dark exhibited optimum stability, while cells stored in outdoor conditions degrades faster, and encapsulated solar cells stored outdoor condition could be completely dead within a month due to external environmental effects light sunlight exposure. Besides, some electrodes like silver undergo accelerated decomposition reactions in the outdoor conditions [6]. Different researches have been conducted using different metal oxide transport layers to promote the performance and stability of perovskite solar cells by changing the thickness of the absorber layer [33–35]. Many researchers used different mechanisms to increase the stability PSCs, and achieved some promising results [35, 36]. However, some of the researches are carried out under indoor controlled conditions, which cannot be viable for commercial applications; the performance, and stability achieved in outdoor conditions can still be improved by changing the device architecture, and passivation defects.

In this work, outdoor performance and stability of cesium containing triple-cation perovskite solar cells in Bahir Dar climatic conditions have been studied. The work encompasses the J-V sweep of the device under dark conditions, forward scan, reverse scan, and cyclic scan under outdoor solar radiation illumination of encapsulated devices and steady-state PL measurements. As an extension, the proposed and ongoing work aims to improve the performance and stability of perovskite solar cells by changing the device architecture.

2 Materials and Methods

2.1 Device Preparation

All chemicals were purchased from Sigma-Aldrich, unless stated otherwise. Fluorine doped tin oxide coated glass slides were cleaned by sonication in 2% Hellmanex solution for 15 min. The substrate was cleaned with deionized water and ethanol followed by sonication with acetone and isopropanol for 15 min each. It was then further treated with UV ozone for 15 min directly before compact layer deposition.

TiO_2 compact layer was deposited by spray pyrolysis from a precursor solution consisting of 0.4 ml acetylacetonate, 0.6 ml titanium diisopropoxide bis (acetylacetonate) and 9ml ethanol at 450 °C. After cooling down to room temperature, mesoporous TiO_2 was deposited by spincoating TiO_2 paste (150 mg/ml in ethanol, Greatcell Solar) at 4000 rpm for 20 s, followed by annealing at 450 °C for 30 min. Substrates were cooled down to 150 °C and immediately transferred to a nitrogen filled glovebox for perovskite deposition. Mixed halide cation perovskite films were deposited from a precursor solution containing FAI (1 M, Greatcell Solar), PbI_2 (1.1 M, TCI), MABr (0.2 M, Greatcell

Solar), $PbBr_2$ (0.2 M, TCI) and CsI (0.075 M) in anhydrous DMF:DMSO 4:1 (v:v). The perovskite solution was spin-coated using a two-step program, 1000 and 6000 rpm for 10 and 20 s respectively. While carrying out the second spin coating step 200 μl of chlorobenzene was dripped on the spinning substrate 5 s before the end of the program. The substrates were then treated with heat by annealing at 100 °C for 1 h in a nitrogen glove box. Subsequently, the substrates were cooled down for a few minutes and a Spiro-OMeTAD (Merck) solution (70 mM in chlorobenzene) doped with bis (trifluoromethylsulfonyl)imide lithium salt (Li-TFSI), tris(2-(1H-pyrazol-1-yl)-4-tert-butylpyridine)-cobalt(III)tris(bis(trifluoromethylsulfonyl)imide) (FK209, Dyenamo) and 4-tert-butylpyridine (TBP) was spincoated at 4000 rpm for 20 s. The compositional molar ratio of additives to spiro-OMeTAD were: 0.5, 0.03 and 3.3 for Li-TFSI, FK209 and TBP, respectively. Finally, 70 nm of gold was thermally evaporated under high vacuum on top of the HTM [11, 12, 15, 27, 29, 37]. Ten identical encapsulated devices/samples were prepared from the same composition. The basis for selecting these compositions is to promote stability without significantly affecting the performance. If the concentration of inorganic components high, it will significantly affect the performance.

2.2 Device Characterisation

The J-V characteristics of the devices were performed using Keithley 2400 source meter with I-V tracer software under dark conditions, and the outdoor environment under ambient Bahir Dar climatic conditions. The samples were nominally identical replicates labeled as 1 to 7. The devices numbers 1, 2 & 4 are not included in the illumination result. The first sample was used for dark current measurement and familiarisations for indoor measurements using mercury lamps; the second sample was damaged during the measurement, fourth sample electrode was difficult to locate its detection because of its encapsulation.

The incident power illuminated on the device is regularly measured with a lux meter which detects light in the visible spectral range. Its measurements are converted into mW/cm^2 using the 1-sun (100 mW/cm^2) radiation as a standard factor to include the UV-spectrum of the solar radiation. There is no readily available standard conversion between solar irradiance and Lux. In this report, solar Irradiance of 1 Sun (1,000 W/m^2) equals approximately 120,000 lx which was developed based on measurement uncertainties, equipment calibration accuracy, and standards' data conversion factor has been used [38]. Moreover, it was difficult to know when the AM 1.5 equivalent is shining on the solar cell as the measurements in outdoor conditions. This causes some errors on the reported input power radiation and then on the efficiency. The J-V scanning was carried out in the forward scan (from V_{sc} to V_{oc}) and backward scan (from V_{oc} to V_{sc} is) directions as well as single cycle scan (from V_{sc} to V_{oc} and then back to V_{sc}) patterns for the first seven devices. The remaining three Devices were reserved for spectroscopy measurements. Figure 2 depicts the schematic diagram of the J-V characterization of the setup.

Steady-state photoluminescence (PL) spectroscopy emission measurements were performed with an excitation wavelength of 500 nm at a scan rate of 600 nm/min. The peak obtained gives information about the charge carrier recombination rates. Based on

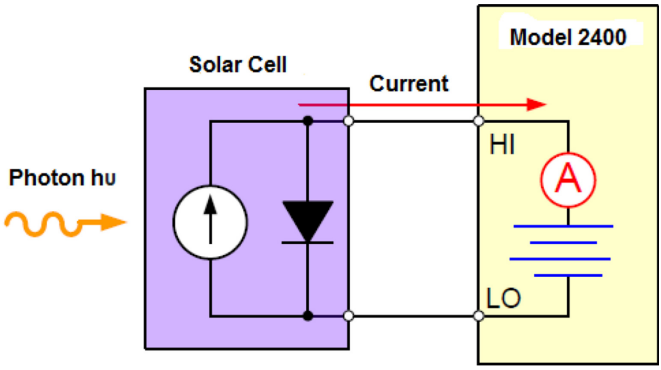

Fig. 2. Schematic diagram of the J-V measurement using Keithely 2400.

the measured values of PL, the performance and stability tests of the encapsulated devices, the following results are obtained.

3 Results and Discussions

3.1 J-V Characteristics of the Device Under Dark Current Measurement

Figure 3 illustrates a representative current-voltage characteristic of the perovskite solar cells. The curve shows that series resistance is low and shunting resistance high, as required for efficient solar cells.

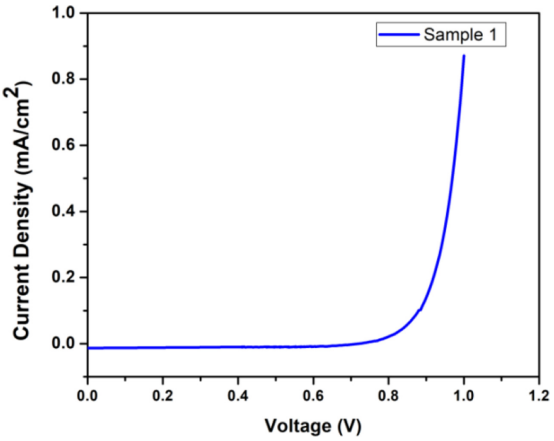

Fig. 3. I-V curve of perovskite device in the dark.

3.2 J-V Sweep of the Device with Outdoor Illuminations, Forward and Reverse Scans (from 12 PM–1 PM)

Figure 4 shows the J-V sweep of Sample 7 under outdoor illumination. The sweep scan is performed in the forward direction (a) and reverses direction (b) by scanning the voltage and measuring the current of the source meter at a scan speed of 40 mV/s. The results show that the device has a performance of 16.80% in the forward scan direction and 14.32% in the backward scan direction. Still there might be errors arising from the estimation of the conversion between solar irradiance and Lux meter as well as the active area. The discrepancy of the curve confirms slight device hysteresis.

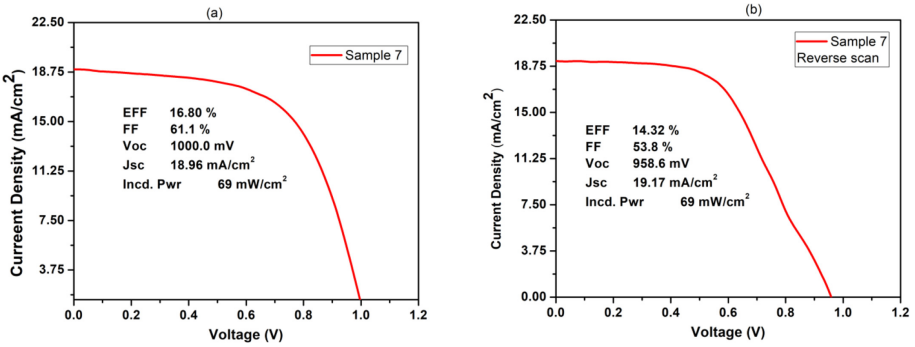

Fig. 4. (a) Forward and (b) reverse J-V scans under outdoor illumination

3.3 J-V Sweep of the Device with Outdoor Illuminations, Cycle Scan (from 12 PM–1 PM)

The curves in Fig. 5 show the one-cycle scan of Sample 3 (a) and 7 (b) under outdoor testing conditions. It was observed that after a careful scan, the source meter is in the off state with output in an open circuit scheme measurements. The performance of the J-V sweep of the device shows that the device demonstrates hysteresis manifested by lack of curve overlap and variation of solar cell parameters. The differences observed in the two curves are due to the presence of mobile ions and trap states. Mobile ions can cause change in the crystal structure and hence the difference of the observation of defects tolerance of the halide perovskites. The trap states affect the diffusion of charge carriers by restricting the mobility of these carriers. The effect and categorisation of the devices were based on the measured values performed repeatedly in the indoor controlled environment.

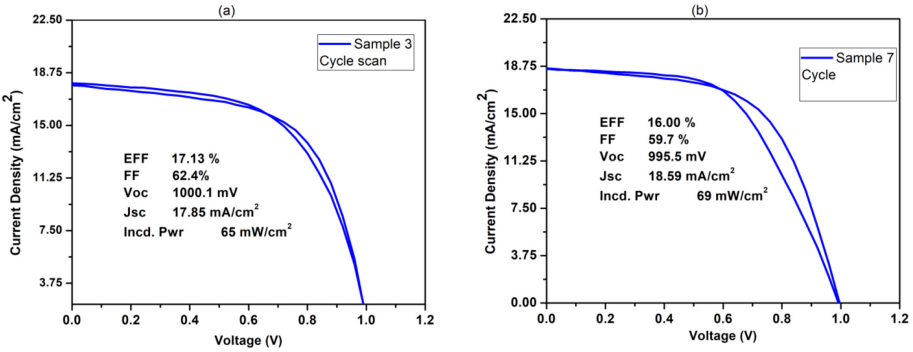

Fig. 5. Cyclic scan (a) sample-3 and (b) sample-7 of the same devices under outdoor illumination.

3.4 Device Performance and Stability Test Summary

Table 1 shows the performance and reproducibility test of 4 identical devices. The measurements were conducted from 28th January to 2nd February 2021 from 11 AM-3 PM. The results obtained a large variability in solar cell parameters, except for V_{oc}. The variability in J_{sc} may be explained by varying climatic conditions and slight variations in the active area size.

Table 1. Performance and reproducibility test (averages)

Sample	Scan Direction	Eff. (%)	FF (%)	Voc (V)	Jsc (mA/cm^2)	I_{in} (mW/cm^2)
Sample 3	Forward	16.3	61.3	1.00	17.3	65
Sample 3	Backward	15.1	55.4	0.98	18.0	65
Sample 5	Forward	13.4	47.1	0.97	19.1	65.14
Sample 5	Backward	10.5	56.4	1.00	18.6	100
Sample 6	Forward	17.2	61.9	1.00	17.0	100
Sample 6	Backward	13.7	57.2	0.97	17.1	100
Sample 7	Forward	14.2	52.7	1.00	16.7	62
Sample 7	Backward	13.6	51.8	0.99	16.5	62

3.5 Steady State Photoluminescence Spectroscopy

Figure 6 displays the steady-state PL emission spectra of the perovskite device as a function of wavelength using a deuterium lamp at an excitation wavelength of 500 nm. The result indicates the existence of strong emission at 757 nm (1.64eV). The emissions peak has been a Gaussian line shape with full width at half maximum (FWHM) of 45 nm resolution.

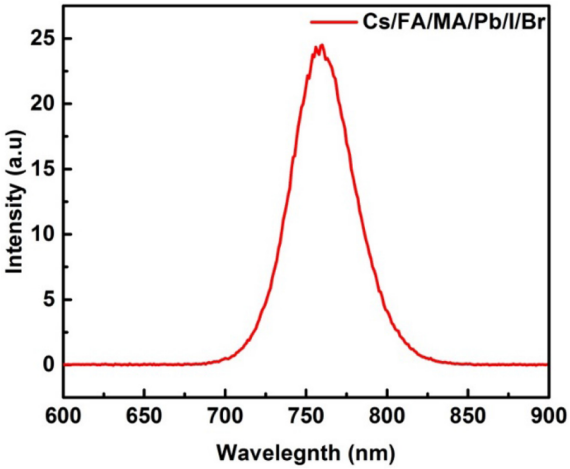

Fig. 6. Steady state PL measurement of encapsulated devices using deuterium lamp.

4 Conclusions and Future Work

In this study, a PCE of more than 16% is obtained, while researches used a baseline PCE of less than 17% with similar composition, but different concentration under indoor illumination [27]. It has been observed that the photovoltaic important solar cell parameters change with aging time. The PCE of the device under investigation changes under continuous illumination of the solar radiation. Sudden changes of the incident solar radiation due to cloud become a bottleneck to clearly articulate the degree of stability. While changing the scan directions, during the J–V measurements, the solar cell parameters changes, and the sweep shows a discrepancy between the forward and reverse scans, and hysteresis is observed in the cyclic scan which indicates that trap states and mobile ions are present in the device. The emission peak of the device has been studied using steady-state PL measurements and observed at that 758 nm. The results of our study are in agreement with other works performed [15, 29]. The triple cation concentration used in the preparation of the device, and its J-V characterization in the uncontrolled real outdoor environment in Bahir Dar climatic condition has not been done so far is the novelty of the work. Our future work will be monitoring the light intensity by continuously measuring the incident radiations using a lux meter/pyranometer to address variable outdoor conditions. By measuring operation continuously including in cloud events, working on extracting important information about how the cells respond **to shading** and then bounce back again will be the tasks to be carried out. Ideally, the device shall be left running for periods of weeks and track data the whole time to study the interrelationship between temperature and band-gap energies on the outdoor performance of device.

Testing the performance using a solar simulator to see its reproducibility with the outdoor measurements will be part of the work included in the package. The work will include treatments with additives to see their impact on the devices hysteresis and longer-term stability and explain the materials change after the operation. The work will be extended to synthesis/fabrication of the devices using optimum characterisation conditions and appropriate additives as well as assessing the potential of the techno-economic analysis of manufacturing the device locally.

Acknowledgements. The work is supported by **Engineering and Physical Sciences Research Council for (EPSRC), UK for Affordable Perovskite Solar Irrigation Systems for Small-holder Farmers in Ethiopia (APSISSFE), EPSRC Reference no EP/T02030X/1. Thus, the authors are** grateful the EPSRC for their financial support.

References

1. Yurui, M.Z., Ke, X., Lin, R., Luo, X., Han, Q., Tan, H.: Recent progress in the developing efficient monolithic all-perovskite tandem solar cells. J. Semicod. **41** 051201 (2020)
2. Zhao, Y., Ma, F., Gao, F., Yin, Z., Zhang, X., You, J.: Research progress in large-area Perovskite solar cells. Photonics Res. **8**, A1–A15 (2020)
3. Park, N.-G., Zhu, K.: Scalable fabrication and coating methods for perovskite solar cells and solar modules. Nat. Mate. **5**, 333–350 (2020)
4. Zhao, B.: Efficient light-emitting diodes from mixed-dimensional perovskites on a fluoride interface. Nat. Electron. **3**, 704–710 (2020)
5. Chen, J., Park, N.-G.: Causes and solutions of recombination in perovskite solar cells (2018)
6. Chauhan, A.K., Kumar, P.: Degradation in perovskite solar cells stored under different environmental conditions. Phys. D Appl. Phys. **50** 325105 (2017)
7. Idoko, L., Anaya-Lara, O., McDonald, A.: Enhancing PV modules efficiency and power output using multi-concept cooling technique. Energy Rep. **4**, 357–369 (2018)
8. Qiab, B., Wang, J.: Fill factor in organic solar cells. Phys. Chem. Chem. Phys. **15**, 8972 (2013)
9. Hossain, M.I., Qarony, W., Ma, S., Zeng, L.: Perovskite/Silicon tandem solar cells: from detailed balance limit calculations to photon management. Nano-Micro Lett. **11**, 58 (2019)
10. Green, M.A., Ho-Baillie, A., Snaith, H.J.: The emergence of perovskite solar cells. Nat. Phtonics **8**, 506–514 (2014)
11. Stranks, S.D., Snaith, H.J.: Perovskite Solar Cells (2016)
12. Olaleru, S.A., Kirui, J.K., Wamwangi, D., Roro, K.T., Mwakikunga, B.: Perovskite solar cells: the new epoch in photovoltaics. Solar Energy **196**, 295–309 (2020)
13. Ahmed, M.I., Habib, A., Javaid, S.S.: Perovskite solar cells: potentials, challenges, and opportunities (2015)
14. Chen, Y., Zhang, L., Zhang, Y., Gaoa, H., Yan, H.: Large-area perovskite solar cells – a review of recent progress and issues. Royal Soc. Chem. **8**, 10489–10508 (2018)
15. Tang, H., He, S., Peng, C.: A short progress report on high-efficiency perovskite solar cells. Nanoscale Res. Lett. **12**, 410 (2017)
16. Tennyson, E.M., Doherty, T.A..S., Stranks, S.D.: Heterogeneity at multiple length scales in halide perovskite semiconductors. Nat. Revi. Mater. **4**, 573–587(2019)
17. De Wolf, S., et al.: Organometallic halide perovskites: sharp optical absorption edge and its relation to photovoltaic performance. J. Phys. Chem. Lett. **5**(6), 1035–1039 (2014)

18. Lozano, G.: The role of metal halide perovskites in next-generation lighting devices. J. Phys. Chem. Lett. **20148**(9), 3987–3997 (2014)
19. Stranks, S.D.: Electron-hole diffusion lengths exceeding 1 Micrometer in an Organometal Trihalide Perovskite Absorber. Science **342**(6156), 341–344 (2013)
20. Sivula, K.: Are organic semiconductors viable for robust, high-efficiency artificial photosynthesis? ACS Energy Lett. **5**(6), 1970–1973 (2020)
21. Juarez-Perez, E.J., Ono, L.K., Maeda, M., Jiang, Y., Hawash, Z., Yabing, Q.: Photodecomposition and thermal decomposition in methylammonium halide lead perovskites and inferred design principles to increase photovoltaic device stability, J. Mater. Chem. A **6**, 9604 (2018)
22. Barker, F.A.J., et al.: Defect-assisted photoinduced halide segregation in mixed-halide perovskite thin. ACS Energy Lett. **2**(6), 1416–1424 (2017)
23. Stranks, S.D., Nayak, P.K., Zhang, W., Stergiopoulos, T., Snaith, H.J.: Formation of thin films of organic-inorganic perovskites for high-efficiency solar cells. Angew. Chem. Int. Ed. **54**(11), 3240–3248 (2015)
24. Howard, J.M., Tennyson, E.M. Neves, B.R.A., Leite, M.S.: Machine learning for perovskites' reap-rest-recovery cycle. Joule **3**, 325–337 (2019)
25. Chen, B., Rudd, P.N., Yang, S., Yuan, Y., Huang, J.: Imperfections and their passivation in halide perovskite solar cells. Chem. Soc. Rev. **48**, 3842 (2019)
26. Mahapatra, A., Parikh, N., Kumar, P., Kuma, M.: Changes in the electrical characteristics of perovskite solar cells with aging time. Molecules **25**, 2299 (2020)
27. Saliba, M.: Cesium-containing triple cation perovskite solar cells: improved stability, reproducibility and high efficiency (2016)
28. Abdi-Jalebi1, M., et al.: Charge extraction via graded doping of hole transport layers gives highly luminescent and stable metal halide perovskite devices. Friend Sci. Adv. **5**, eaav2012 (2019)
29. Jain, S.M., et al.: Vapor phase conversion of PbI2 to CH3NH3PbI3: spectroscopic evidence for formation of an intermediate phase. J. Mater. Chem. A **4**, 2630–2642 (2013)
30. Liu, Z., et al.: A holistic approach to interface stabilization for efficient perovskite solar modules with over 2,000-hour operational stability, Nat. Energy **5**, 596–604 (2020)
31. Mica, N.A.: Triple-cation perovskite solar cells for visible light communications. Photonics Res. **8**, A16–A24 (2020)
32. Ašmontas, S., et al.: Cesium-containing triple cation perovskite solar cells, coatings (2021)
33. Ghosh, A., Dipta, S.S., Shafaat Saud Nikor, S.K., Saqib, N., Saha, A.: Performance analysis of an efficient and stable perovskite solar cell and a comparative study of incorporating metal oxide transport layers. J. Opt. Soc. Am. B 37, 1966–1973 (2020)
34. PriyankaRoy, A.: Analysis of an efficient and eco-friendly $CsGeSnI_3$ based perovskite solar cell: a theoretical study. Materials Today **44**, 2997–3000 (2021)
35. Kheralla, A., Chetty, N.: A review of experimental and computational attempts to remedy stability issues of perovskite solar cells. Heliyon **7**, e06211 (2021)
36. Aydin, E., et al.: Interplay between temperature and bandgapenergies on the outdoor performance of perovskite/silicon tandem solar cells. Nat. Energy **5**, 851–859 (2020)
37. Baena, J.P.C., et al.: Highly efficient planar perovskite solar cells through band alignment engineering. Energy Environ. Sci. **8**, 2928–2934 (2015)
38. Micheal, P.: A conversion guide: solar irradiance and lux illuminance (2020)